第51卷第6期 中国科学技术大学学报 Vol. 51, No. 6
2021年6月 JOURNAL OF UNIVERSITY OF SCIENCE AND TECHNOLOGY OF CHINA Jun. 2021
Received: 2021-05-06; Revised: 2021-06-05 doi:10.52396/JUST-2021-0123

Transit-time scattering of radiation belt electrons by off-equatorially generated magnetosonic waves

WU Zhiyong[1,2], SU Zhenpeng[1,2]*
1. CAS Key Laboratory of Geospace Environment, Department of Geophysics and Planetary Sciences, University of Science and Technology of China, Hefei 230026, China;
2. CAS Center for Excellence in Comparative Planetology, Hefei 230026, China
* Corresponding author. E-mail: szpe@mail.ustc.edu.cn

Abstract: In the inner magnetosphere, the magnetosonic waves have been proposed to transit-time scatter the radiation belt electrons over a broad range of energy and pitch-angle. Recent observations have shown that magnetosonic waves can be generated in the off-equatorial plasmasphere, whose latitudinal coverage and propagation angle are significantly different from the traditional magnetosonic waves confined near the equator. Using our previously-developed test-particle code, we here investigate the possible transit-time scattering of radiation belt electrons by the off-equatorially generated magnetosonic waves. Our results indicate that the transit-time scattering is primarily related to the perturbation near the edge of the finite wave train. The extending of wave occurrence latitudes causes the shrinking of the equatorial pitch-angle range of the transit-time scattering. Compared to the near-equatorially confined magnetosonic waves, the off-equatorially generated magnetosonic waves produce ignorable pitch-angle perturbations but slightly stronger energy perturbations.

Keywords: magnetosonic wave; radiation belt; transit-time scattering
CLC number: P354 **Document code**: A

1 Introduction

Magnetosonic waves are the low-frequency, highly-compressional electromagnetic emissions in the inner magnetosphere. About 50 years ago, Russell et al.[1] firstly reported the magnetosonic waves on the basis of OGO 3 observations. In recent years, these waves have received increased attention for their potential contribution to the radiation belt electron dynamics. Horne et al.[2] showed that magnetosonic waves can cause Landau resonant acceleration of electrons between ~10 keV and several MeV in the outer radiation belt. Shprits[3] proposed the bounce-resonance between magnetosonic waves and radiation belt electrons. Bortnik et al.[4] suggested the transit-time scattering of radiation belt electrons by the near-equatorially confined magnetosonic waves. Along with these theoretical insights above, a number of observational studies have linked the radiation belt electron dynamics, such as the formation of electron butterfly distributions[5-9], to the concurring magnetosonic waves.

The efficiency of all the three mechanisms mentioned above depends on the latitudinal coverage and propagation angle of magnetosonic waves. In previous studies, the magnetosonic waves are usually considered to be generated by the ion Bernstein mode instability at the quasi-perpendicular normal angle near the equator[10-13]. In the numerical calculations[14,15], these waves are assumed to be confined within ±3° latitude away from the magnetic equator. Recent observations and ray-tracing simulations[16] have found that the off-equatorial ion Bernstein mode instability can produce magnetosonic waves near the plasmapause. Compared to the traditional near-equatorially generated magnetosonic waves, these off-equatorially generated waves can bounce over a broader range of latitude and have normal angles further away from 90°. How the off-equatorially generated magnetosonic waves affect the radiation belt electrons remains unclear.

In this study, we perform test-particle simulations to investigate the transit-time scattering of radiation belt electrons by magnetosonic waves. We show that, compared to the near-equatorially confined magnetosonic waves, the off-equatorially generated magnetosonic waves produce the ignorable pitch-angle perturbations but the slightly stronger energy

Citation: WU Zhiyong, SU Zhenpeng. Transit-time scattering of radiation belt electrons by off-equatorially generated magnetosonic waves. J. Univ. Sci. Tech. China, 2021, 51(6): 453-458.

perturbations.

2 Magnetosonic wave properties

Figure 1 presents a revisit of the magnetosonic waves observed by Van Allen Probe A on 2013-08-13[16]. These waves appeared as a band of enhanced electromagnetic emissions centering at the local lower hybrid resonance frequency $f_{\rm lhr}^{\rm RBSP}$, qualitatively different from the traditional magnetosonic waves below the lower hybrid resonance frequency. According to the cold plasma wave dispersion relation, these waves extending above the lower hybrid resonance frequency should have normal angles far away from 90°. Such normal angles allow the magnetosonic waves propagate along the magnetic field lines toward higher latitudes than the observer's latitude of ~15°.

Our previous linear instability analyses[16] have shown that these magnetosonic waves mainly grow at latitudes >15° when the normal angles have moved close to 90°. The subsequent ray-tracing simulations[16] further confirmed that these waves initialized with the "appropriate" normal and azimuthal angles can accumulatively gain energy from the hot protons over latitudes $|\lambda|<30°$ during the bounce-drift process inside the plasmasphere. As shown in Figure 2(a), the magnetosonic wave power peaked at ~170 Hz around 19:30 UT. Figure 2(b) demonstrates the normal-angle variations along the latitude for the 170 Hz wave with the "super gain" during bounce-drift propagation[16]. The normal angle ψ is about 85° at $\lambda=0°$, and increases to ~90° at $\lambda\approx25°$. The latitudinal dependence of normal angle can be approximately written as

$$\psi = 1.4877674 + 0.43245313\lambda^2 \quad (1)$$

where both ψ and λ are in unit of radian. We next investigate the transit-time scattering of radiation belt electrons by this monochromatic wave of 170 Hz.

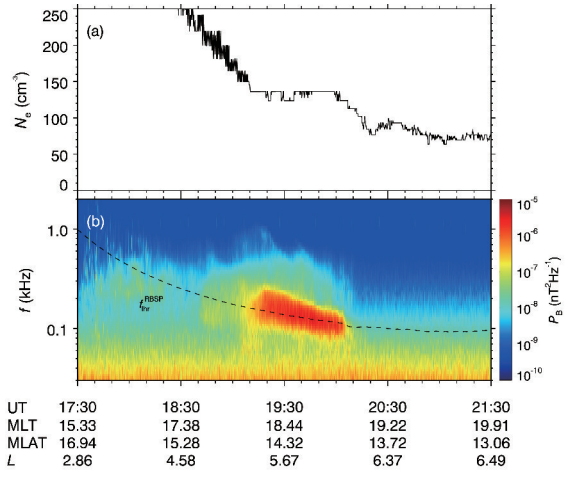

Figure 1. Van Allen Probes observation of magnetosonic waves generated off-equatorially in the high-density plasmasphere[16]: (a) cold electron density N_e; (b) wave magnetic power spectral density P_B.

3 Test-particle simulations

We use the full test-particle code developed by Su et al[17] to investigate the interaction between magnetosonic waves and radiation belt electrons. This full test-particle code is an improved version of the early gyro-averaged test-particle code[18-20]. With this full test-particle code, there have been a series of studies of nonlinear interactions between electromagnetic ion cyclotron waves and magnetospheric particles[21,22]. For an arbitrary particle with the charge q, rest mass m, Lorentz factor γ, position vector $\boldsymbol{r}$ and relativistic momentum vector $\boldsymbol{p}$, its trajectory is determined by the following equations:

$$\frac{\mathrm{d}\boldsymbol{r}}{\mathrm{d}t} = \frac{\boldsymbol{p}}{\gamma m} \quad (2)$$

$$\frac{\mathrm{d}\boldsymbol{p}}{\mathrm{d}t} = q\left[\boldsymbol{E}_w + \frac{\boldsymbol{p}}{\gamma m}\times(\boldsymbol{B}_0+\boldsymbol{B}_w)\right] \quad (3)$$

To exclude the azimuthal drift of the test-particle, the background magnetic field $\boldsymbol{B}_0$ is simplified as a "magnetic bottle" in the Cartesian coordinate system[23-26]:

$$\boldsymbol{B}_0 = -\frac{x}{2}\frac{\mathrm{d}B_D}{\mathrm{d}z}\boldsymbol{e}_x - \frac{y}{2}\frac{\mathrm{d}B_D}{\mathrm{d}z}\boldsymbol{e}_y + B_D\boldsymbol{e}_z \quad (4)$$

$$B_D = \frac{B_E}{L^3}\frac{\sqrt{1+3\sin^2\lambda}}{\cos^6\lambda},\ B_E = 31200\ \mathrm{nT} \quad (5)$$

$$\frac{\mathrm{d}z}{\mathrm{d}\lambda} = R_E L\cos\lambda\sqrt{1+3\sin^2\lambda} \quad (6)$$

with the z-component to be equal to the original Earth's magnetic field magnitude depending on L and λ, and the additionally introduced x- and y-components to

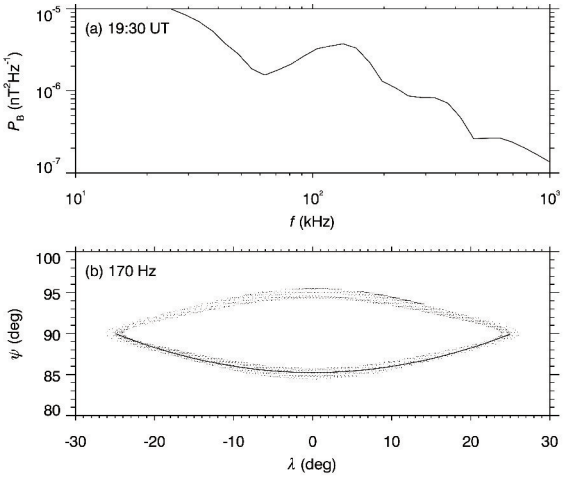

Figure 2. Magnetosonic wave properties around 19:30 UT: (a) frequency-dependent magnetic power spectral density P_B; (b) latitude-dependent normal-angle ψ of 170 Hz wave from the previous ray-tracing simulations (dots)[16] and from the polynomial model (line).

maintain the divergence-free condition. Because the x- and y-components are much weaker than the z-component, this model can reproduce the characteristic of wave-particle interaction in the realistic dipole field. For an arbitrary wave, the angular frequency ω, wave vector $\boldsymbol{k}=k\sin\psi\boldsymbol{e}_x+k\cos\psi\boldsymbol{e}_z$ and normal angle ψ obey the well-known cold-plasma wave dispersion relation[27]. Its electromagnetic fields are listed as follows:

$$\boldsymbol{E}_w = -E_w^x\sin\phi\boldsymbol{e}_x - E_w^y\cos\phi\boldsymbol{e}_y - E_w^z\sin\phi\boldsymbol{e}_z \quad (7)$$

$$\boldsymbol{B}_w = B_w^x\cos\phi\boldsymbol{e}_x - B_w^y\sin\phi\boldsymbol{e}_y + B_w^z\cos\phi\boldsymbol{e}_z \quad (8)$$

with the wave phase angle

$$\phi(t,x,z) \equiv \int\boldsymbol{k}\cdot\mathrm{d}\boldsymbol{r} - \int\omega\mathrm{d}t \quad (9)$$

According to the observations in Figure 1[16], we perform the test-particle simulations at $L=5.7$ in a dipole field. We have taken into account the latitudinal dependence of background electron density[28]

$$N_e = N_{eq}\cos^{-2\eta}\lambda \quad (10)$$

with the latitudinal index $\eta=0.5$ and the equatorial density $N_{eq}=115\ \mathrm{cm}^{-3}$. We select a monochromatic magnetosonic wave of 170 Hz, whose normal angle varies with latitude (Equation (1)). The wave magnitude is assumed to be

$$B_W = B_{W0}\frac{[1-\tanh(\frac{\lambda-\lambda_{max}}{\Delta\lambda})][1+\tanh(\frac{\lambda+\lambda_{max}}{\Delta\lambda})]}{4} \quad (11)$$

with $B_{W0}=20$ pT and $\Delta\lambda=0.02$ rad. Specifically, $B_W\approx B_{W0}$ when $|\lambda|<\lambda_{max}$; B_W drops down toward zero when $|\lambda|\sim\lambda_{max}$; $B_W=0$ when $|\lambda|>\lambda_{max}$.

Figure 3 presents the variations in the equatorial pitch-angle and energy of electrons under the action of the magnetosonic wave confined near the equator ($\lambda_{max}=3°$). The counter-streaming and co-streaming interactions correspond to the situations of $\boldsymbol{k}\cdot\boldsymbol{p}<0$ and $\boldsymbol{k}\cdot\boldsymbol{p}>0$. All the test-electrons are initialized with the energy of $E_k=0.1$ MeV and the equatorial pitch-angle $\alpha_{eq}=30°$, and their initial gyro-phases are uniformly distributed in the range of $0-2\pi$. In the high density plasmasphere, the wave parallel phase velocity is much smaller than the electron parallel velocity. For both counter-streaming and co-streaming interactions, the test electrons have experienced the perturbations of waves in about 10 periods. In each full wave period, the non-resonant perturbations average to zero. The net variations of pitch-angle and energy are essentially related to the perturbation near the edge of the finite wave train. Specifically, the net variations in the pitch-angle and energy for both situations are comparable: $\Delta\alpha_{eq}\approx0.002°$ and $\Delta E_k\approx0.25$ eV.

In Figure 4, we have enlarged the latitudinal range of magnetosonic waves by setting $\lambda_{max}=23°$. Clearly, compared to the near-equatorially confined magnetosonic waves, the off-equatorially generated magnetosonic waves have caused the slightly higher energy variation ΔE_k but ignorable pitch-angle variation $\Delta\alpha_{eq}\approx0.0002°$. In our simulation, the wave magnetic field amplitude is assumed to be constant at latitudes $|\lambda|<\lambda_{max}$. As the latitude increases, the background magnetic field and then the wave electric field increases. Hence, the non-resonant perturbation in energy tends to increase. As discussed in our previous work[17], the gyro-averaged change rate of the equatorial pitch angle $\mathrm{d}\alpha_{eq}/\mathrm{d}t$ is inversely proportional

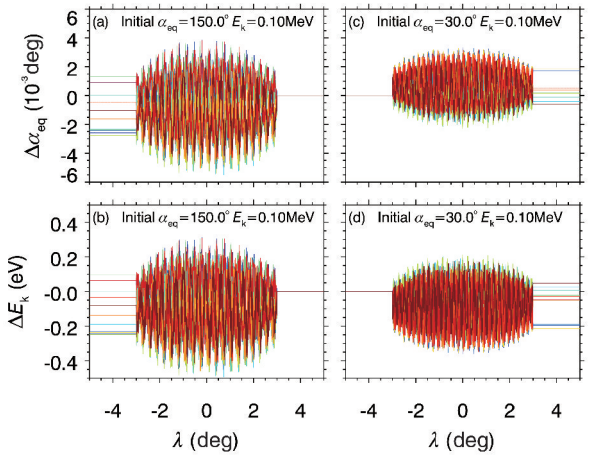

Figure 3. Counter-streaming (left) and co-streaming (right) scattering of radiation belt electrons by magnetosonic waves confined within $|\lambda|\leqslant3°$: (a, c) equatorial pitch-angle change $\Delta\alpha_{eq}$; (b, d) kinetic energy change ΔE_k. The lines are color-coded according to the initial gyro-phase of test particles.

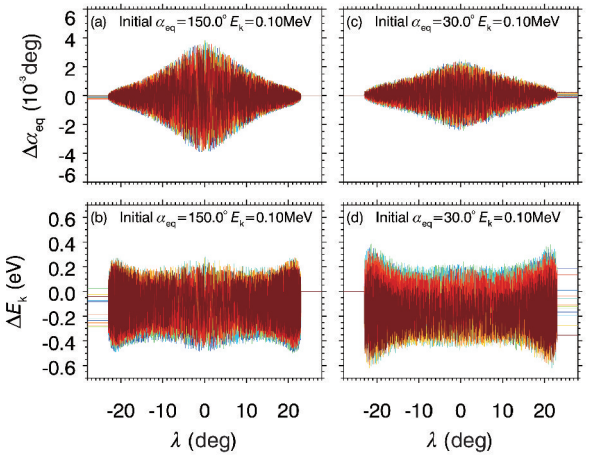

Figure 4. Counter-streaming (left) and co-streaming (right) scattering of radiation belt electrons by magnetosonic waves confined within $|\lambda|\leqslant23°$: (a, c) equatorial pitch-angle change $\Delta\alpha_{eq}$; (b, d) kinetic energy change ΔE_k. The lines are color-coded according to the initial gyro-phase of test particles.

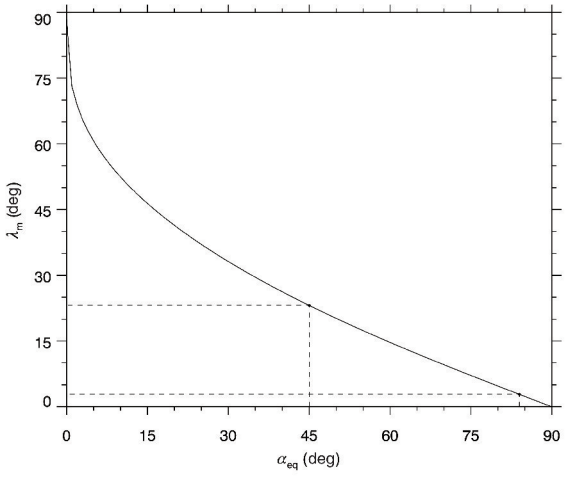

Figure 5. Dependence of mirror latitude λ_m on equatorial pitch-angle α_{eq}.

to tan α, with the local pitch-angle α. At higher latitudes, the local pitch-angle α moves closer to 90° and the resulted non-resonant perturbation of α_{eq} is weaker.

Figure 5 plots the dependence of the mirror latitude λ_m on the equatorial pitch-angle α_{eq}. For the electrons always in the field of wave train, the non-resonant perturbations would not accumulate. To experience the accumulative, non-resonant, transit-time scattering, the electrons have to go through the edges of the wave train. Clearly, the electrons with larger α_{eq} have lower λ_m. For $\lambda_{max}=3°$ and 23°, the corresponding thresholds are $\alpha_{eq} \approx 83°$ and 45°. In other words, with the occurrence latitude λ_{max} of magnetosonic waves extending from 3° to 23°, the equatorial pitch-angle range of the transit-time scattering shrinks from $\alpha_{eq}<83°$ to $\alpha_{eq}<45°$.

4 Conclusions

Our recent study[16] has illustrated the generation of magnetosonic waves by the off-equatorial hot protons inside the plasmapause. We here investigate the transit-time scattering of radiation belt electrons by such off-equatorially generated magnetosonic waves. The main results are listed as follows:

(Ⅰ) In the high-density plasmasphere, the so-called transit-time scattering is related to the non-resonant perturbations near the edge of the wave train. In response to the extension of wave occurrence latitude from 3° to 23°, the equatorial pitch-angle range of transit-time scattering shrinks from <83° to <45°.

(Ⅱ) Compared to the near-equatorially confined magnetosonic waves, the off-equatorially generated magnetosonic waves cause the ignorable equatorial pitch-angle perturbations but the slightly larger energy perturbations.

Our present simulations are based on a specific event of magnetosonic waves generated off-equatorially[16]. The change of wave characteristics and background conditions would alter the perturbations in both pitch-angle and energy. For simplicity, our present model includes only a monochromatic wave, rather than a group of waves representing the observed magnetosonic band. As shown in our simulations, the transit-time scattering is mainly related to the non-resonant perturbations near the edge of the wave train. A superposition of many waves would not qualitatively change the picture, and a quantitative study is left for future.

Acknowledgments

We acknowledge the EMFISIS team for the use of Van Allen Probes data (http://emfisis.physics.uiowa.edu/Flight/). This work is supported by the Strategic Priority Research Program of Chinese Academy of Sciences (XDB 41000000), the National Natural Science Foundation of China (41774170 and 41631071).

Conflict of interest

The authors declare no conflict of interest.

Author information

WU Zhiyong is currently a doctoral candidate at University of Science and Technology of China. He received the BS degree from China University of Geosciences (Wuhan) in 2019. His current research interests focus on the generation, propagation and evolution of plasma waves in inner magnetosphere of Earth.

SU Zhenpeng (corresponding author) is a professor at CAS Key Laboratory of Geospace Environment, Department of Geophysics and Planetary Sciences, University of Science and Technology of China (USTC). He received his PhD degree in geophysics from USTC in 2011. His research interests include space plasma physics, magnetospheric physics and planetary science. He was awarded the Excellent Young Scientists Foundation of the National Natural Science Foundation of China in 2014. He has published more than 80 scientific papers with over 2200 citations.

References

[1] Russell C T, Holzer R E, Smith E J. OGO 3 observations of ELF noise in the magnetosphere. 2. The nature of the equatorial noise. J. Geophys. Res., 1970, 75: 755-768.

[2] Horne R B, Thorne R M, Glauert S A, et al. Electron acceleration in the Van Allen radiation belts by fast magnetosonic waves. Geophys. Res. Lett., 2007, 34: L17107.

[3] Shprits Y Y. Potential waves for pitch-angle scattering of near-equatorially mirroring energetic electrons due to the violation of the second adiabatic invariant. Geophys. Res. Lett., 2009, 36: L12106.

[4] Bortnik J, Thorne R M. Transit time scattering of energetic electrons due to equatorially confined magnetosonic waves. J. Geophys. Res., 2010, 115: A07213.

[5] Fu S, Ni B, Li J, et al. Interactions between magnetosonic waves and ring current protons: Gyroaveraged test particle simulations. Journal of Geophysical Research (Space Physics), 2016, 121: 8537-8553.
[6] Li J, Bortnik J, Thorne R M, et al. Ultrarelativistic electron butterfly distributions created by parallel acceleration due to magnetosonic waves. Journal of Geophysical Research (Space Physics), 2016, 121: 3212-3222.
[7] Li J, Ni B, Ma Q, et al. Formation of energetic electron butterfly distributions by magnetosonic waves via Landau resonance. Geophys. Res. Lett., 2016, 43: 3009-3016.
[8] Yang C, Su Z, Xiao F, et al. A positive correlation between energetic electron butterfly distributions and magnetosonic waves in the radiation belt slot region. Geophys. Res. Lett., 2017, 44: 3980-3990.
[9] Ni B, Zou Z, Fu S, et al. Resonant scattering of radiation belt electrons by off-equatorial magnetosonic waves. Geophys. Res. Lett., 2018, 45: 1228-1236.
[10] Gulelmi A V, Klaine B I, Potapov A S. Excitation of magnetosonic waves with discrete spectrum in the equatorial vicinity of the plasmapause. Planet. Space Sci., 1975, 23: 279-286.
[11] Curtis S A, Wu C S. Gyroharmonic emissions induced by energetic ions in the equatorial plasmasphere. J. Geophys. Res., 1979, 84: 2597-2607.
[12] Boardsen S A, Gallagher D L, Gurnett D A, et al. Funnel-shaped, low-frequency equatorial waves. J. Geophys. Res., 1992, 97: 14967-14976.
[13] Chen L, Thorne R M, Jordanova V K, et al. Global simulation of magnetosonic wave instability in the storm time magnetosphere. J. Geophys. Res., 2010, 115: A11222.
[14] Bortnik J, Thorne R M, Ni B, et al. Analytical approximation of transit time scattering due to magnetosonic waves. Geophys. Res. Lett., 2015, 42: 1318-1325.
[15] Ma Q, Li W, Thorne R M, et al. Electron scattering by magnetosonic waves in the inner magnetosphere. Journal of Geophysical Research (Space Physics), 2016, 121: 274-285.
[16] Wu Z, Su Z, Liu N, et al. Off-equatorial source of magnetosonic waves extending above the lower hybrid resonance frequency in the inner magnetosphere. Geophysical Research Letters, 2021, 48: e2020GL091830.
[17] Su Z, Zhu H, Xiao F, et al. Latitudinal dependence of nonlinear interaction between electromagnetic ion cyclotron wave and terrestrial ring current ions. Phys. Plasmas, 2014, 21: 052310.
[18] Su Z, Zhu H, Xiao F, et al. Bounce-averaged advection and diffusion coeffificients for monochromatic electromagnetic ion cyclotron wave: Comparison between test-particle and quasi-linear models. J. Geophys. Res., 2012, 117: A09222.
[19] Zhu H, Su Z, Xiao F, et al. Nonlinear interaction between ring current protons and electromagnetic ion cyclotron waves. J. Geophys. Res., 2012, 117: A12217.
[20] Su Z, Zhu H, Xiao F, et al. Latitudinal dependence of nonlinear interaction between electromagnetic ion cyclotron wave and radiation belt relativistic electrons. J. Geophys. Res., 2013, 118: 3188-3202.
[21] Wang B, Su Z, Zhang Y, et al. Nonlinear Landau resonant scattering of near-equatorially mirroring radiation belt electrons by oblique EMIC waves. Geophys. Res. Lett., 2016, 43(8): 3628-3636.
[22] Wang G, Su Z, Zheng H, et al. Nonlinear fundamental and harmonic cyclotron resonant scattering of radiation belt ultrarelativistic electrons by oblique monochromatic EMIC waves. Journal of Geophysical Research (Space Physics), 2017, 122: 1928-1945.
[23] Inan U S, Bell T F, Helliwell R A. Nonlinear pitch angle scattering of energetic electrons by coherent VLF waves in the magnetosphere. J. Geophys. Res., 1978, 83: 3235-3253.
[24] Bell T F. The nonlinear gyroresonance interaction between energetic electrons and coherent VLF waves propagating at an arbitrary angle with respect to the earth's magnetic field. J. Geophys. Res., 1984, 89: 905-918.
[25] Bortnik J, Thorne R M, Inan U S. Nonlinear interaction of energetic electrons with large amplitude chorus. Geophys. Res. Lett., 2008, 35: L21102.
[26] Tao X, Bortnik J. Nonlinear interactions between relativistic radiation belt electrons and oblique whistler mode waves. Nonlinear Processes in Geophysics, 2010, 17: 599-604.
[27] Stix T H. Waves in Plasmas. New York: American Institute of Physics, 1992.
[28] Denton R E, Goldstein J, Menietti J D. Field line dependence of magnetospheric electron density. Geophys. Res. Lett., 2002, 29: 2205.

非赤道区域激发的磁声波对辐射带电子的渡越时间散射效应

吴志勇[1,2], 苏振鹏[1,2]*

1. 中国科学技术大学地球物理与行星科学系中科院近地空间环境重点实验室, 安徽合肥 230026;
2. 中国科学院比较行星学卓越创新中心, 安徽合肥 230026
* 通讯作者. E-mail: szpe@mail.ustc.edu.cn

摘要: 在内磁层中, 磁声波被认为能够通过渡越时间散射影响很大能量以及投掷角范围的辐射带电子. 近期观测研究发现, 磁声波可以在等离子体层内的非赤道区域被激发并且在纬度覆盖范围、法向角变化等方面都与传统的赤道区域磁声波有显著不同. 利用之前发展的试验粒子模型, 我们研究了非赤道磁声波对辐射带电子的渡

越时间散射效应.发现该效应主要发生在波列的边缘.波动纬度覆盖范围的扩展造成了该效应的有效赤道投掷角范围的收缩.相比于赤道区域磁声波,非赤道激发的磁声波可以产生更强的能量扰动以及可忽略的投掷角扰动.

关键词:磁声波;辐射带;渡越时间散射